# Adsorption of He atoms in external grooves of single-wall carbon nanotube bundles

Antonio Šiber*
*Institute of Physics, P.O. Box 304, 10001 Zagreb, Croatia*
(Received 28 June 2002; published 14 November 2002)

I calculate the quantum states for He atom in the potential of an external groove of the single-wall carbon nanotube bundle. The calculated ground-state energy is found to be in fair agreement with the experimental estimate which suggests that the outer groove site is a preferential site for the adsorption of He gas in the samples studied experimentally. I also calculate the specific heat of low-density $^4$He atom gas adsorbed in groove positions. The specific geometry of the groove and its influence on the adsorbate quantum states and specific heat are discussed.

DOI: 10.1103/PhysRevB.66.205406 PACS number(s): 65.80.+n, 68.43.De, 68.65.−k

## I. INTRODUCTION

Recent thermal desorption[1–3] and specific heat[4,5] experiments on nanotube samples have detected $^4$He atoms adsorbed in these samples. These experiments have attracted attention due to the potential application of the carbon nanotube materials for an efficient storage of gases.[6–8] In this respect, it is important to know the details of the adsorption process and the preferential adsorption sites. It is still not clear whether He atoms adsorb in the interstitial channels between the close-packed nanotubes within a bundle or in the external groove positions of the bundle[6,8] (see Fig. 1). For open-end tubes, He atoms could also adsorb within the tubes.[9] The thermal desorption experiments reported in Ref. 1 were first successfully interpreted by assuming that He atoms occupy the interstitial channels,[1] while later reevaluation of the experimental data[2] led authors of Ref. 3 to put forth the proposition that He atoms adsorb in the external grooves of the nanotube bundle. Measurements of adsorption isotherms for heavier gases (Xe, $CH_4$, and Ne)[10] yielded that these gases do not adsorb in the interstitial channels but probably in the external grooves. By comparing their results for heavier gases with with the data for $^4$He,[1,2] the authors of Ref. 10 concluded that $^4$He atoms most probably adsorb also in the external groove positions. The experimentally determined[2] ground state energy of $^4$He ($-19.8 \pm 1.5$ meV)[11] is significantly higher than the ground state energy calculated for $^4$He atom adsorbed in the nanotube interstitial channel ($-27.8$ meV in Ref. 12, $-29.1$ meV in Ref. 7, and $-33.3$ meV in Ref. 8). This indeed suggests that He atoms may be adsorbed in the external groove positions. The theoretical estimate for the ground state energy of $^4$He atoms adsorbed in the external groove[8] is -23.3 meV, still somewhat lower from the experimental estimate. It is therefore of interest to examine the details of adsorption of He atoms in the groove positions, in particular the influence of very specific geometry of the groove position (see Fig. 2) on the bound state energies of He adsorbate.

The measurements of specific heat of He adsorbates in the nanotube samples could be of help to resolve the adsorption site dilemma. In this respect, it should be of use to compare the theoretical predictions for the specific heat with the experimental data. The theoretical prediction for the specific heat of low density (noninteracting) $^4$He gas adsorbed in the interstitial channels has been presented in Ref. 12. In this article I shall consider the adsorption of He atoms in the external grooves of nanotube bundle and calculate the specific heat for the low-density gas of noninteracting He adsorbates.

The outline of the article is as follows. In Sec. II, the interaction potential confining the He adsorbate to the bundle external groove is discussed. In Sec. III, I shortly present a method of coupled channels which is used to solve the single-particle Schrödinger equation in a potential of the groove. A short description of the application of the method to the specific geometry of the groove is given. The energies of quantum states of the adsorbate are calculated together with the corresponding wave functions. In Sec.IV, the quantum specific heat of $^4$He atoms adsorbed in the groove positions is calculated. The results of the article are summarized in Sec. V.

## II. ADSORPTION POTENTIAL FOR HE ATOM ON THE OUTER SURFACE OF THE BUNDLE

In Fig. 1, a bundle containing 37 nanotubes is sketched. The external groove and the interstitial channel adsorption sites, together with the choice of the coordinate system are denoted. This figure suggests that the total He-bundle inter-

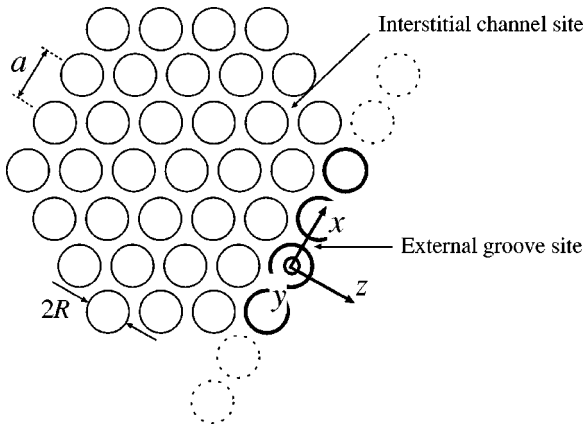


FIG. 1. Geometry of the bundle of carbon nanotubes with designations of the external groove and interstitial channel adsorption sites and a choice of coordinate system.

 

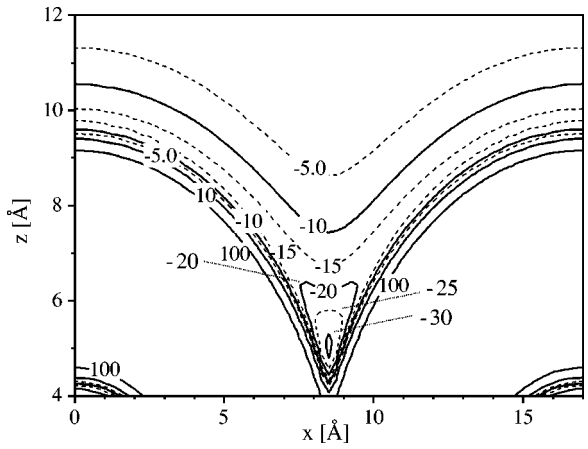


FIG. 2. The interaction potential (in meV) for He adsorbate in the external groove region. The centers of the two tubes surrounding the groove are positioned at $x=0.0$ Å, $z=0.0$ Å and $x=17.0$ Å, $z=0.0$ Å.

action potential, $V_t(x,y,z)$ can be obtained as a sum of He-tube interactions $V(\mathbf{r}-\mathbf{r}_n)$,

$$V_t(\mathbf{r})=\sum_n V(\mathbf{r}-\mathbf{r}_n), \tag{1}$$

where $\mathbf{r}=(x,y,z)$ and $\mathbf{r}_n$ are the radius vectors of He atom and the tube (labeled with index $n$), respectively. The He-tube interaction potential can in principle be obtained as a sum of effective He-C interactions.[6–9,12] The thus obtained He-tube potential would therefore exhibit corrugation along the tube resulting from a discrete nature of the tube material. In what follows, I shall neglect the corrugation of the He-tube potential. This approximation effectively ''smears'' the carbon atoms to obtain a homogeneous smooth tube surface. The same approximation has been invoked in Refs. 7–9, but not in Ref. 12. I shall later discuss the impact of this assumption on final results.

It has been shown in Ref. 9 that in the approximation of a smooth nanotube, the He-single wall nanotube potential can be represented as

$$V(\rho)=3\pi\theta\epsilon\sigma^2\left[\frac{21}{32}\left(\frac{\sigma}{R}\right)^{10}\eta^{11}M_{11}(\eta)-\left(\frac{\sigma}{R}\right)^{4}\eta^{5}M_5(\eta)\right], \tag{2}$$

where $\epsilon$ and $\sigma$ are the energy and range parameter of the effective He-C interaction assumed to be of a Lennard-Jones form. Variable $\rho$ is the distance of the He atom from the tube axis, $\theta$ is the effective coverage of C atoms on a tube surface ($0.381/\text{Å}^2$), $R$ is the tube radius and variable $\eta$ is defined as $\eta=R/\rho$ when $\rho>R$, which is a case of interest to this work. Function $M_n(\eta)$ is defined as

$$M_n(\eta)=\int_0^{\pi}\frac{d\phi}{(1+\eta^2-2\eta\cos\phi)^{n/2}}. \tag{3}$$

If the bundle is very large, the potential for He atom on the surface of the bundle is almost periodic in the $x$ direction (Fig. 1), due to the fact that there is a large number of tubes forming a ''flat'' side of the bundle (the tubes denoted by thick line circles in Fig. 1). This suggests that we can write the total He-bundle potential as a Fourier series

$$V_t(\mathbf{r})=\sum_G V_G(z)\exp(iGx), \tag{4}$$

where $G=2n\pi/a$, $n$ is integer, and $a$ is the distance between the two neighboring tube axes as denoted in Fig. 1. Note that the total potential does not show dependence on the $y$ coordinate due to the fact that the tube discrete nature has been neglected. By using Eq. (1) in Eq. (4), and neglecting interactions of He atom with all tubes lying below the bundle side (which are vanishingly small due to a large diameter of carbon nanotubes), it is straightforward to show that the Fourier components of the total potential $V_G(z)$ are given as

$$V_G(z)=\frac{2}{a}\int_0^{\infty}V(\sqrt{x^2+z^2})\cos(Gx)dx. \tag{5}$$

The total potential obtained from Eqs. (4) and (5) exhibits complete two-dimensional periodicity, i.e., it represents an infinitely long bundle side, as suggested by the dashed circles in Fig. 1. It is clear that the assumed periodicity of the bundle side has no effect on the bound state energy at all, since it is determined only by the two tubes surrounding a groove. Even for higher bound states, the assumption of the potential periodicity does not affect the eigen energies. This is again due to large diameter of carbon nanotubes.

In what follows, I shall concentrate on (10,10) single wall nanotubes of the so-called ''armchair'' type.[13] The parameters of effective Lennard-Jones He-C site potential I use are $\epsilon=1.45$ meV and $\sigma=2.98$ Å. These parameters were obtained from the so-called combination rules[16] and were also used in Ref. 8. The He-tube potential obtained from Eq. (2) using the tube radius of $R=6.9$ Å has a well depth of $-15.64$ meV, and its minimum is positioned at $\rho=9.85$ Å. The total potential [Eq. (1)] is plotted in Fig. 2 within the unit cell of the infinite bundle side. The size of the unit cell is $a=2R+3.2$ Å$=17$ Å, in agreement with experimentally determined tube-tube separation.[14]

The expression for the He-tube potential in Eq. (2) is not convenient to calculate the Fourier transforms in Eq. (5) in analytic fashion. In this respect, I have found that the potential in Eq. (2) can be represented with excellent accuracy in the whole region of $\rho$ coordinate where the potential is smaller than $\sim 400$ meV as

$$V(\rho)=A_1\exp[-\beta_1(\rho-\rho_0)]-A_2\exp[-\beta_2(\rho-\rho_0)], \tag{6}$$

with a set of parameters $A_1=3.4$ meV, $A_2=18.81$ meV, $\beta_1=5.22$ 1/Å, $\beta_2=0.892$ 1/Å, and $\rho_0=9.85$ Å. Note that $\rho_0$ is not an independent parameter of this potential. It was introduced simply to scale the values of $A_1$ and $A_2$ parameters to an acceptable range. In our choice of coordinate system $\rho=\sqrt{x^2+z^2}$. The functional form of the He-tube potential in Eq. (6) results in analytic expressions for the Fourier components

$$V_G(z)=\frac{2}{a}\left[A_1\exp(\beta_1\rho_0)\frac{\beta_1 z}{\sqrt{G^2+\beta_1^2}}K_1(z\sqrt{G^2+\beta_1^2})\right.$$
$$\left.-A_2\exp(\beta_2\rho_0)\frac{\beta_2 z}{\sqrt{G^2+\beta_2^2}}K_1(z\sqrt{G^2+\beta_2^2})\right], \tag{7}$$

where $K_1$ is the modified Bessel function of first order.[15] Note that the problem of He adsorption in external grooves has been effectively reduced to the problem of He adsorption on a very corrugated surface made of carbon nanotubes. This enables us to use the techniques developed to treat the problem of adsorption on surfaces.[16]

## III. SOLUTION OF THE SCHRÖDINGER EQUATION IN THE POTENTIAL OF THE GROOVE

The single-particle Schrödinger equation for a He atom in the groove potential can be written as

$$-\frac{\hbar^2}{2M}\nabla^2\Psi(\mathbf{r})+V_t(\mathbf{r})\Psi(\mathbf{r})=E\psi(\mathbf{r}), \tag{8}$$

where $\Psi(\mathbf{r})$ is the wave function of the adsorbate, $M$ and $E$ are its mass and energy, respectively. The symmetry of the potential suggests that one can write the wave function in the form

$$\Psi(\mathbf{r})=\exp(iK_y y)\sum_G \xi_G(z)\exp[i(K_x+G)x], \tag{9}$$

where the two-dimensional adsorbate wave vector in the $(x,y)$ plane is denoted by $\mathbf{K}=(K_x,K_y)$. Substituting Eqs. (9) and (4) in Eq. (8) one obtains a set of coupled linear differential equations for functions $\xi_G(z)$,

$$\left(\frac{d^2}{dz^2}+k_G^2\right)\xi_G(z)-\frac{2M}{\hbar^2}\sum_{G'} V_{G-G'}(z)\xi_{G'}(z)=0. \tag{10}$$

Here,

$$k_G^2=\frac{2ME}{\hbar^2}-K_y^2-(K_x+G)^2. \tag{11}$$

The set of equations (10) typically occurs in scattering problems[17–20] where the equations (the so-called coupled channel equations[20]) are to be solved with a requirement that $\xi_G(z)$ functions reduce to asymptotic scattering solutions in the region where the interaction vanishes. In our case, we are interested in states which vanish in the region where the potential has extremely large values and also in the region where the potential itself vanishes (bound states). To solve these equations for bound states, I adopt the procedure described in Ref. 17. Basically, one numerically propagates the matrix of $\xi_G(z)$ functions, (the log-derivative method of Johnson[18] is used for the propagation), from the region of large and small $z$ coordinate and requires that the matrix of solutions matches smoothly at some predefined coordinate $z_{fix}$. By systematically varying energy $E$ for fixed $K_x$, it is possible to determine all the bound state energies of the system.[17] Varying additionaly the value of $K_x$, one can obtain the whole energy spectrum of the adsorbate. In a log-derivative scheme for solving these equations, one actually does not propagate the wave functions $[\xi_G(z)]$ and their derivatives with respect to $z$ coordinate $[\xi_G'(z)]$, but a combination of type $\xi_G'(z)/\xi_G(z)$,[20,17] the so-called log-derivative matrix. In this way one avoids problems associated with the propagation of solutions in classically highly forbidden regions,[20,17] which is very important in our case since the region of the groove is surrounded with highly repulsive, classically forbidden regions (see Fig. 2). The details of this procedure for the geometry of interest here have been developed in Ref. 19. It should be noted that the procedure used here to solve the Schrödinger equation is not the same as the one presented in Ref. 12 and used for a potential of the interstitial channel. In the case of the interstitial channel potential, a much simpler scheme for the calculation of bound states was used, due to the fact that the potential in that case has much higher symmetry.[12]

The total energy of the adsorbate can be written as

$$E=\frac{\hbar^2K_y^2}{2M}+E_m(K_x,K_y=0), \tag{12}$$

so that it is sufficient to consider only $K_y=0$ case in solving equations (10). The index $m$ represents the adsorbate ''bands'' obtained as solutions of Eqs. (10) with $K_y=0$.

It can be shown that the density of adsorbate bound states can be written as

$$\rho_{2D}(E)=\sqrt{\frac{2M}{\hbar^2}}\frac{2L_xL_y}{(2\pi)^2}\sum_m\int_0^{\pi/a}dK_x\frac{\Theta[E-E_m(K_x,K_y=0)]}{\sqrt{E-E_m(K_x,K_y=0)}}, \tag{13}$$

where $L_x$ and $L_y$ are the dimensions of the normalization box in $x$ and $y$ directions, respectively, and $\Theta$ is the Heaviside step function. Assuming that the solutions do not show appreciable dispersion with $K_x$, i.e., that $E_m(K_x,K_y=0)\approx E_m(K_x=0,K_y=0)=E_m$, for the density of states one can write

$$\rho_{2D}(E)=\sqrt{\frac{2M}{\hbar^2}}N_x\frac{L_y}{2\pi}\sum_m\frac{\Theta(E-E_m)}{\sqrt{E-E_m}}, \tag{14}$$

where $N_x$ is the number of tubes in the bundle side. Equation (14) is obviously a simple sum of effectively one-dimensional densities of states for a single groove, reflecting a situation where the adsorbate atom is strongly localized in a particular groove region. It is therefore natural in this case to define a density of states per unit length for a *single* groove as

$$g(E)=\frac{1}{L_yN_x}\rho_{2D}(E). \tag{15}$$

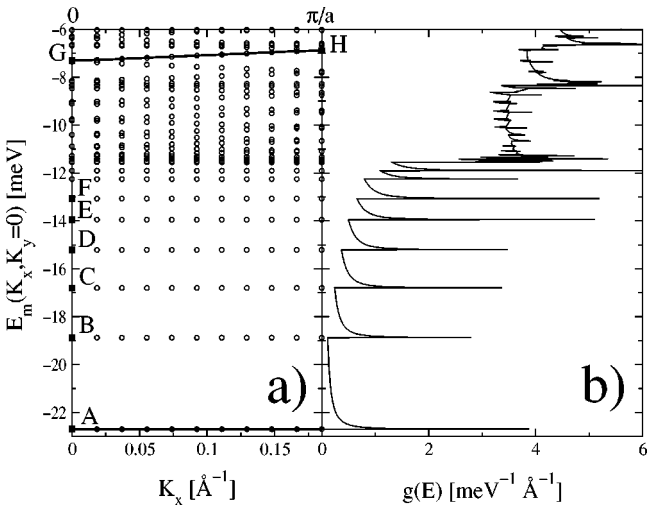


FIG. 3. (a) Energy bands for $^4$He adsorbate in an external groove of a bundle consisting of (10,10) nanotubes. The empty circles represent the actually calculated points. The lowest energy band and the band connecting G and H states have been drawn (full lines). (b) The corresponding density of states calculated from Eqs. (15) and (13).

The potential in Fig. 2 cannot be accurately represented with small number of Fourier components. This is due to the fact that the groove region is very small on the scale of lattice constant *a*. For example, the equipotential contour of -30 meV has a mean radius of about 0.2 Å. I have found that about 77 Fourier components with $G=\pm n2\pi/a$, $n=0,1,\ldots,38$ are needed to represent the total potential with an excellent accuracy in the whole region of importance.

In Fig. 3(a), the energy bands of a $^4$He adsorbate are plotted. Note that the ''bands'' up until $\sim -11$ meV are indeed nearly dispersionless, so that approximation for the density of states in Eq. (14) holds with great accuracy in that interval of energies. In Fig. 3(b) the density of states obtained from Eq. (15) is plotted [the details of band dispersion are included, i.e., Eq. (15) in combination with Eq. (13) is used]. As expected from the geometry of the groove, the phase space is much larger for higher He energies which is clear from the increase of the density of states at about $-10$ meV, an effect that is evident in Fig. 3(b). For higher energies, the adsorbate becomes less confined to the groove region and the energy levels become denser. The actual magnitude of the density of states per unit length of a groove should be compared with the one obtained in Ref. 12 (Fig. 2 of that reference) for He adsorbed in an interstitial channel. From this comparison, it is evident that the He atom is significantly less confined in a groove region than in the interstitial channel region. This was of course expected prior to any calculations. It is also visible in Fig. 3 that the typical elements of the band structure calculations appear for bound state energies higher than $\sim -11$ meV, where the bands acquire dispersion, which means that the probability of finding the adsorbate in the region of a neighboring groove rises for these energies. It is also interesting to note that the density of states becomes nearly constant (as a function of energy) for energies between about $-11$ and $-8$ meV, which is typical

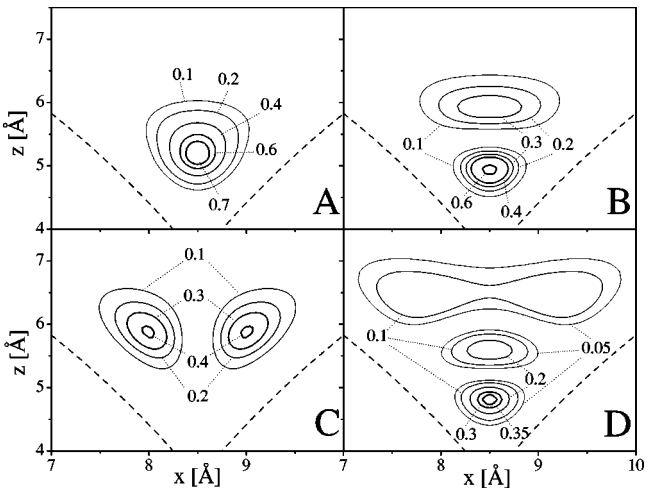


FIG. 4. The probability density functions of the states denoted by A, B, C, and D in Fig. 3. The dashed lines represent the 100 meV equipotential contour of the He-bundle potential.

for the adsorbates nearly free in two dimensions.[16] Thus, a transition from the effectively one-dimensional adsorbate for low energies to effectively two-and-more-dimensional adsorbate for higher energies, is evident in the density of states.

Although the effects discussed in a previous paragraph can be traced in the adsorbate density of states, it would certainly be of use to visualize the wave functions of the adsorbate. The log-derivative method can be used to yield a precise information on the wave function.[17] In Figs. 4 and 5, we plot the probability densities of the states denoted by letters from A–H in Fig. 3. The probability density, $P_m(x,z;K_x)$, for a quantum state in a band *m*, characterized additionally with a wave vector $\mathbf{K}=(K_x,K_y)$ is defined as

$$P_m(x,z;K_x)=|\Psi_m(x,y,z;K_x)|^2, \tag{16}$$

and the wave functions are normalized according to

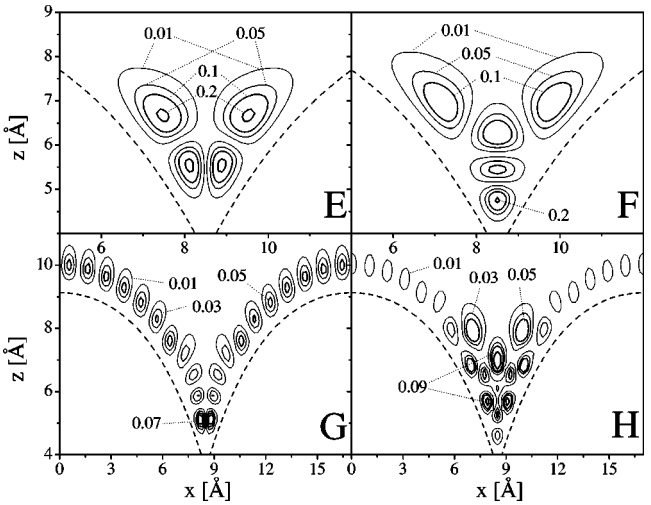


FIG. 5. The probability density functions of the states denoted by E, F, G, and H in Fig. 3. The dashed lines represent the 100 meV equipotential contour of the He-bundle potential. Note the different scales of *x* and *z* axes in upper and lower panels.

$$\int_0^a dx \int_0^\infty dz |\Psi_m(x,y,z;K_x)|^2 = 1. \tag{17}$$

Note that the probability density does not depend on the $y$ coordinate and $y$ component of the wave vector.

From Fig. 4 it can be seen that the higher energy states become more delocalized in $x$, but most notably in the $z$ direction, i.e., the probability of finding an adsorbate atom in a region of large $z$ coordinate rises with bound state energy. The dashed lines in Figs. 4 and 5 denote the 100 meV equipotential contour of He-bundle interaction (see Fig. 2). It is interesting to note that for states G and H (two lower panels of Fig. 5), the probability density function becomes significantly delocalized over the whole surface of the bundle. This reflects a highly delocalized adsorbate which is not strongly confined to the groove region.

Occupation of the positions on the bundle surface and away from the restricted region of the groove as a function of gas pressure has been predicted in Ref. 21 for Ar adsorbates. In that case, as the gas pressure rises, the coverage of the adsorbed gas increases in almost discrete steps and the bundle surface eventually becomes covered by a striped monolayer film. Upon further increase in pressure, a bilayer adsorbate film forms. It should be emphasized that the change of effective adsorbate dimensionality observed in this article is a quantum effect related to a change of behavior of the single particle wave function as the adsorbate bound state energy increases. Thus, this effect is most easily observed as the sample temperature increases and the occupation of excited bound states becomes probable. Similar effect has been predicted for quantum gases adsorbed inside single-wall carbon nanotubes.[9,22] In that case, thermal excitation of the azimuthal modes[9] causes transition from 1D to 2D behavior of adsorbates.

The ground state energy of $^4$He atom in a groove is $E_\Gamma = -22.7$ meV, in fair agreement with an experimental estimate[2,3] ($-19.8 \pm 1.5$ meV), and significantly higher from the ground state energy of $^4$He atom in an interstitial channel ($-27.9$ meV).[12] It is of interest now to examine the effect of the details of the potential on the lowest bound state energy. In this respect, for the effective He-C site potential, we adopt a slightly different set of parameters, used in Ref. 12 and obtained from the analysis of data on helium atom scattering from graphite[23] ($\epsilon = 1.34$ meV and $\sigma = 2.75$ Å). This set of parameters results in the ground state energy of $-17.1$ meV, which is in somewhat better agreement with the experimental estimate. Interestingly enough, relatively small change in the He-C binary potential parameters results in a large change of ground state energy. This is due to a pronounced sensitivity of the shape and magnitude of the total potential in the region where the ground state is localized (see panel A of Fig. 4) on the details of the binary potential. It is reasonable to expect that a more refined He-tube potential would yield a better agreement with the experimental estimate. It is also possible that an inclusion of corrugation in the potential along the $y$ direction would produce a somewhat lower ground state energy, as has been observed for He adsorption on graphite surface.[24]

## IV. SPECIFIC HEAT OF $^4$He ATOMS ADSORBED IN THE EXTERNAL GROOVES

As shown in Ref. 12, the isosteric specific heat $C/N$ of low-density, noninteracting adsorbate gas, significantly delocalized in one dimension ($y$ coordinate in our case), can be obtained from

$$\frac{C}{N} = L_y \frac{k_B}{(k_B T)^2} \frac{I_2 - I_1^2/I_0}{N}, \tag{18}$$

where $N$ is the number of the adsorbate atoms within a *single* external groove, $T$ is the sample temperature, $k_B$ is the Boltzmann constant, and the integral quantities $I_j$ are defined as

$$I_j = \int_{E_\Gamma}^\infty g(E) E^j \exp\left[\frac{E-\mu(T)}{k_B T}\right] f^2(E,T) dE, \quad j = 0,1,2. \tag{19}$$

Here $E_\Gamma$ is the lowest allowed adsorbate energy (point A in Fig. 3), $\mu(T)$ is the chemical potential of the system obtained from the requirement of the adsorbate number conservation,[12,24] and $f(E,T)$ is the Bose-Einstein distribution function

$$f(E,T) = \frac{1}{\exp\left(\frac{E-\mu}{k_B T}\right) - 1}. \tag{20}$$

The same equations appropriate for adsorption on surfaces have been derived in Ref. 24. Note that when Eq. (15) in combination with Eq. (13) is used, Eq. (18) correctly accounts for the delocalization of the adsorbate in the $x$ direction.

The present approach does not treat He-He interactions. Our results are therefore not applicable to the whole range of temperatures and He atom concentrations. For temperatures not so low and concentrations not so high that the He-He interactions dominate the specific heat, this approach should yield accurate results. A virial expansion approach to treat the He-He interactions for He atoms adsorbed on graphite surface has been described in Ref. 25.

Figure 6 shows the results for the isosteric specific heat of the adsorbate gas as a function of sample temperature and for three different linear densities ($N/L_y$) of adsorbates along the groove. All three curves in Fig. 4 are very similar to each other but very different from the corresponding curves when $^4$He atoms are assumed to occupy interstitial channel positions (Figs. 3 and 4 of Ref. 12). The difference is a consequence of the fact that the He adsorbate in a groove becomes effectively two dimensional for lower sample temperature due to the fact that it is less efficiently confined than in the case of adsorption in interstitial channel. The observed difference also suggests that the measurements of the specific heat of the low density He gas adsorbed in nanotube samples could be used to determine the relevant He adsorption sites. The results for the specific heat are expected to be less sensitive to the corrugation of the potential than in the case of the interstitial channel adsorption.[12] This is simply due to the fact that the adsorbate is not completely surrounded by nano-

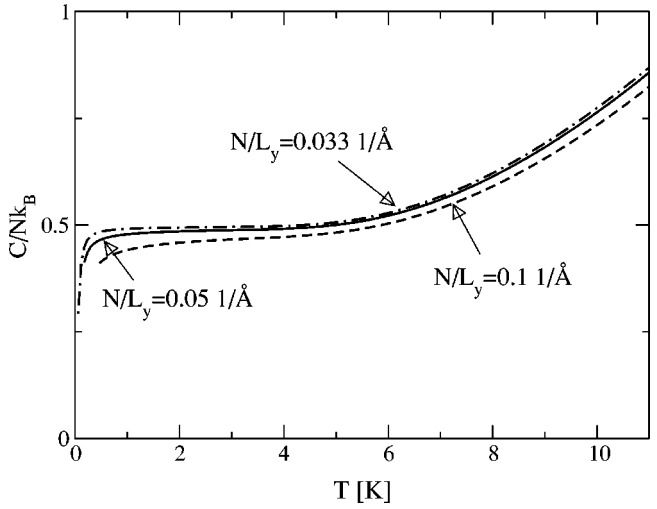


FIG. 6. Isosteric specific heat of a noninteracting gas of $^4$He atoms adsorbed in external groove positions for three different adsorbate linear densities. Dash-dotted line: $N/L_y=0.033$ 1/Å, full line: $N/L_y=0.05$ 1/Å, dashed line $N/L_y=0.1$ 1/Å.

tubes. Therefore, the adsorbate wave functions ''sample'' the corrugation in a smaller region of space, particularly for higher energy states which are more extended in the *z* direction. This is very different from the corresponding effect when the adsorbate is localized in the interstitial channel region. In that case, the higher energy states are more strongly influenced by the corrugation due to the fact that their delocalization in the region of the channel cross section induces a larger overlap of the wave function with the corrugated part of the confining potential.

## V. SUMMARY

The ground state energy of $^4$He atom adsorbed in the external groove position has been calculated and found to be in fair agreement with the experimentally determined energy. All the excited states of the adsorbate and the corresponding density of states have been calculated from our approach. From these calculated quantities, we calculated the specific heat of the adsorbate gas in the approximation of the noninteracting adsorbates, applicable to low adsorbate densities. The dependence of specific heat on temperature of the sample is markedly different from the corresponding dependence when the adsorbates are assumed to be in the interstitial channels,[12] which is due to less efficient confinement of the adsorbate in the groove region. The measurements of the specific heat may thus provide an additional argument in favor of the assignment of the external groove position as a preferential adsorption site for He atoms in the experiments performed in Refs. 1–3.

*Email address: asiber@ifs.hr

[1] W. Teizer, R.B. Hallock, E. Dujardin, and T.W. Ebbesen, Phys. Rev. Lett. **82**, 5305 (1999).
[2] W. Teizer, R.B. Hallock, E. Dujardin, and T.W. Ebbesen, Phys. Rev. Lett. **84**, 1844(E) (2000).
[3] Y.H. Kahng, R.B. Hallock, E. Dujardin, and T.W. Ebbesen, J. Low Temp. Phys. **126**, 223 (2002).
[4] J. Hone, B. Batlogg, Z. Benes, A.T. Johnson, and J.E. Fischer, Science **289**, 1730 (2000).
[5] J.C. Lasjaunias, K. Biljaković, Z. Benes, J.E. Fischer, and P. Monceau, Phys. Rev. B **65**, 113409 (2002).
[6] M.M. Calbi, M.W. Cole, S.M. Gatica, M.J. Bojan, and G. Stan, Rev. Mod. Phys. **73**, 857 (2001).
[7] G. Stan, V.H. Crespi, M.W. Cole, and M. Boninsegni, J. Low Temp. Phys. **113**, 447 (1998).
[8] G. Stan, M.J. Bojan, S. Curtarolo, S.M. Gatica, and M.W. Cole, Phys. Rev. B **62**, 2173 (2000).
[9] G. Stan and M.W. Cole, Surf. Sci. **395**, 280 (1997).
[10] S. Talapatra, A.Z. Zambano, S.E. Weber, and A.D. Migone, Phys. Rev. Lett. **85**, 138 (2000).
[11] The experimental uncertainty has been determined from Fig. 2 of Ref. 2.
[12] A. Šiber and H. Buljan, Phys. Rev. B **66**, 075415 (2002).
[13] N. Hamada, S.-I. Sawada, and A. Oshiyama, Phys. Rev. Lett. **68**, 1579 (1992).
[14] A. Thess, R. Lee, P. Nikolaev, H.J. Dai, P. Petit, J. Robert, C.H. Xu, Y.H. Lee, S.G. Kim, A.G. Rinzler, D.T. Colbert, G.E. Scuseria, D. Tomanek, J.E. Fischer, and R.E. Smalley, Science **273**, 483 (1996).
[15] M. Abramowitz and I.A. Stegun, *Handbook of Mathematical Functions, With Formulas, Graphs, and Mathematical Tables* (Dover Publications, New York, 1972).
[16] L.W. Bruch, M.W. Cole, and E. Zaremba, *Physical Adsorption: Forces and Phenomena* (Clarendon Press, Oxford, 1997).
[17] J.M. Hutson, Comput. Phys. Commun. **84**, 1 (1994).
[18] B.R. Johnson, J. Comput. Phys. **13**, 445 (1973).
[19] A. Šiber, Ph.D. thesis, University of Zagreb, 2002. Downloadable at URL http://bobi.ifs.hr/~asiber/PhDThesis/
[20] M.H. Alexander and D.E. Manolopoulos, J. Chem. Phys. **86**, 2044 (1987); D.E. Manolopoulos, Ph.D. thesis, University of Cambridge, 1988.
[21] S.M. Gatica, M.J. Bojan, G. Stan, and M.W. Cole, J. Chem. Phys. **114**, 3765 (2001).
[22] S.M. Gatica, G. Stan, M.M. Calbi, J.K. Johnson, and M.W. Cole, J. Low Temp. Phys. **120**, 337 (2000).
[23] N. Garcia, W.E. Carlos, M.W. Cole, and V. Celli, Phys. Rev. B **21**, 1636 (1980).
[24] W.E. Carlos and M.W. Cole, Phys. Rev. B **21**, 3713 (1980).
[25] R.L. Siddon and M. Schick, Phys. Rev. A **9**, 907 (1974).